Journal of Applied Mathematics and Physics, 2026, 14(8), 2989-3008
https://www.scirp.org/journal/jamp
ISSN Online: 2327-4379
ISSN Print: 2327-4352

Geometric Distortion of Numerical Ranges under Similarity and Metric Similarity

Faith M. Mwangi, Benard M. Nzimbi, Stephen W. Luketero

Department of Mathematics, University of Nairobi, Nairobi, Kenya
Email: mwangifm@uonbi.ac.ke, nzimbi@uonbi.ac.ke, sluketero@uonbi.ac.ke

How to cite this paper: Mwangi, F.M., Nzimbi, B.M. and Luketero, S.W. (2026) Geometric Distortion of Numerical Ranges under Similarity and Metric Similarity. *Journal of Applied Mathematics and Physics*, **14**, 2989-3008.
https://doi.org/10.4236/jamp.2026.148147

Received: July 2, 2026
Accepted: August 18, 2026
Published: August 21, 2026

Abstract

We study the geometric distortion of numerical ranges of complex matrices under similarity and metric similarity transformations, measuring that distortion through the condition number of the transforming matrix. Four results are obtained. First, we prove a two-sided bound on the numerical radius of a similarity transform, expressed in terms of the condition number, and we give an explicit example showing that the corresponding set inclusion of the numerical range into a dilate of the convex hull of the prototype range fails in general: similarity changes the shape of the numerical range, and not merely its size. Second, for two-by-two nilpotent matrices under diagonal similarity, we obtain an exact scale factor, namely the modulus of the ratio of the two diagonal entries, which shows that the conjectured optimal constant in the first result, the condition number itself, is attained. Third, we prove that the unitary factor in a metric similarity leaves the numerical range unchanged, so that metric similarity and ordinary similarity produce identical numerical-range distortion. Fourth, we resolve completely, in the two-by-two case, the question of when the normalized numerical ranges of the two matrices are related by a rotation: this happens precisely when the matrix is nilpotent, or the two numerical ranges coincide, and the rotation angle can then always be taken to be zero. Throughout, the spectrum is preserved while the numerical range is distorted in a manner controlled, but in general not exactly described, by the condition number.

Keywords

Numerical Range, Numerical Radius, Similarity Transformation, Metric Similarity, Condition Number, Geometric Similarity, Similitude, Operator Theory

1. Introduction

The numerical range of a linear operator, introduced independently by Toeplitz

[1] and Hausdorff [2], has become one of the most important tools in operator theory. For an operator T acting on a complex Hilbert space H, the numerical range

$$W(T) = \{\langle Tx, x\rangle : x \in H, \|x\| = 1\}$$

encodes fundamental information about the operator's action, providing a bridge between algebraic properties and geometric structure. Comprehensive treatments can be found in Gustafson and Rao [3] and Halmos [4].

Scope of the paper. Throughout this paper, we work in the finite-dimensional setting: $H \cong \mathbb{C}^n$ with the standard inner product, and all operators are identified with matrices in $M_n(\mathbb{C})$. This restriction matters for the spectral inclusion: for a matrix T, the numerical range $W(T)$ is compact and $\sigma(T) \subseteq W(T)$; for a general bounded operator on an infinite-dimensional Hilbert space, $W(T)$ need not be closed and only the inclusion $\sigma(T) \subseteq \overline{W(T)}$ holds ([3], Section 1.2). All results in Sections 4 - 9 are stated and proved for matrices.

The Toeplitz-Hausdorff theorem [1] [2], which establishes that $W(T)$ is always convex, represents one of the earliest triumphs of functional analysis. The numerical range contains the spectrum $\sigma(T)$ (in the finite-dimensional setting adopted here) and provides bounds on the operator norm through the numerical radius $w(T) = \max\{|z| : z \in W(T)\}$, which satisfies the fundamental inequalities

$$\frac{1}{2}\|T\| \le w(T) \le \|T\|, \tag{1}$$

as established in [3] [4]. Refinements of these inequalities have been studied extensively by Kittaneh [5] and others.

The behavior of numerical ranges under operator transformations reveals deep structural properties. Under unitary equivalence $S = U^* TU$, the numerical range is preserved: $W(S) = W(T)$. This invariance, discussed in [3] [6], reflects the geometric nature of unitary transformations as rotations and reflections of the underlying space. However, the situation becomes considerably more subtle for similarity transformations $S = X^{-1}TX$, where X is merely invertible rather than unitary.

This paper investigates the nature of numerical-range distortion under similarity and the more general metric similarity. While similarity preserves the spectrum [7], it distorts the numerical range in a manner that can be controlled through the condition number of the similarity transformation. We establish rigorous two-sided bounds on the distortion of the numerical radius, extending the circle of ideas around generalized inclusion relations of Goldberg and Straus [8], and, for important special cases, exact formulas. We emphasize at the outset what our bounds do **not** say: the numerical range $W(S)$ is in general not contained in any fixed dilate $\kappa(X)\cdot \mathrm{conv}(W(T))$ of the prototype region (Example 4.1), so the distortion is genuinely a distortion of size and shape, not a radial rescaling.

The study is motivated by applications in numerical analysis, where condition numbers govern the stability of computational algorithms [7] [9], and by connections to the theory of α -isometries and geometric similarity (similitude) in metric spaces [10]. Our prototype-model framework provides a natural geometric language: $W(T)$ serves as a prototype whose size, and in special cases exact shape, determines that of the model $W(S)$.

2. Preliminaries

Throughout, $H=\mathbb{C}^n$ with inner product $\langle\cdot,\cdot\rangle$ linear in the first argument, and $B(H)=M_n(\mathbb{C})$ is the algebra of $n\times n$ complex matrices. Standard references for this section are [3] [4] [7].

2.1. Numerical Range and Its Properties

Definition 2.1. ([3] Definition 1.1.1). For $T\in M_n(\mathbb{C})$, the numerical range is the set

$$W(T)=\left\{\langle Tx,x\rangle : x\in\mathbb{C}^n, \|x\|=1\right\},$$

and the numerical radius is

$$w(T)=\max\left\{|z| : z\in W(T)\right\}=\max_{\|x\|=1}\left|\langle Tx,x\rangle\right|.$$

Since the unit sphere of $\mathbb{C}^n$ is compact, $W(T)$ is a compact subset of $\mathbb{C}$ and the maxima above are attained. The following classical results will be used throughout.

Theorem 2.2 (Toeplitz-Hausdorff, [1] [2]). *For any* $T\in M_n(\mathbb{C})$, *the numerical range* $W(T)$ *is a convex subset of* $\mathbb{C}$.

Theorem 2.3. ([3], Theorem 1.2.1). *For any* $T\in M_n(\mathbb{C})$, *the spectrum satisfies* $\sigma(T)\subseteq W(T)$.

Remark 2.4. Theorem 2.3 is a genuinely finite-dimensional statement. For a bounded operator T on an infinite-dimensional Hilbert space, the correct general inclusion is $\sigma(T)\subseteq\overline{W(T)}$, and the closure cannot be omitted: the unilateral shift S has $\sigma(S)=\overline{\mathbb{D}}$ while $W(S)$ is the open unit disk. This is the reason for the finite-dimensional scope fixed in the Introduction.

Theorem 2.5 (Elliptical range theorem, ([3] Theorem 1.3.1)). *For any* 2×2 *matrix* T *with eigenvalues* λ_1,λ_2, *the numerical range* $W(T)$ *is a* (*possibly degenerate*) *closed elliptical disk with foci at* λ_1 *and* λ_2 *and minor axis of length*

$$b=\sqrt{\operatorname{tr}(T^*T)-|\lambda_1|^2-|\lambda_2|^2}.$$

2.2. Similarity Relations

Definition 2.6 ([7] Chapter 1). Let $S,T\in M_n(\mathbb{C})$ and let $X\in M_n(\mathbb{C})$ be invertible.

1) S and T are *similar*, written $S\sim T$, if $S=X^{-1}TX$.

2) S and T are *unitarily equivalent*, written $S\cong T$, if $S=U^*TU$ for some unitary U.

3) S and T are *metrically similar*, written $S\overset{\text{m.s.}}{\sim}T$, if $S=UX^{-1}TXU^*$ for

some unitary U and positive invertible X.

The chain of implications $S \cong T \Rightarrow S \overset{\text{m.s.}}{\sim} T \Rightarrow S \sim T$ is strict in general. Each relation preserves the spectrum: $\sigma(S)=\sigma(T)$ ([7], Theorem 1.3.20). However, their effects on the numerical range differ fundamentally, as noted in [3] [6].

Definition 2.7 ([7] Section 5.8). The condition number of an invertible $X \in M_n(\mathbb{C})$ is $\kappa(X)=\|X\|\cdot\|X^{-1}\|$.

The condition number satisfies $\kappa(X)\ge 1$, with equality if and only if X is a positive scalar multiple of a unitary matrix [9]. For diagonal matrices $X=\operatorname{diag}(d_1,\cdots,d_n)$ with $d_i \ne 0$ we have $\kappa(X)=\max_i|d_i|/\min_i|d_i|$. Note that $\kappa(cX)=\kappa(X)$ for every scalar $c\ne 0$; the condition number is a scale-invariant quantity, and correspondingly X and cX implement the same similarity transformation.

We shall also need the classical Kantorovich inequality; see [7] (Section 7.4) or [9].

Lemma 2.8 (Kantorovich inequality). *Let* $A\in M_n(\mathbb{C})$ *be positive definite with spectrum contained in* $[a,b]$, $0<a\le b$. *Then for every unit vector* y,

$$\langle Ay,y\rangle\langle A^{-1}y,y\rangle \le \frac{(a+b)^2}{4ab}.$$

2.3. Geometric Similarity

Definition 2.9 ([10]). Two sets $A,B\subset\mathbb{C}$ are *geometrically similar* (or *similitudes*) if there exist $\alpha>0$, $\theta\in[0,2\pi)$, and $c\in\mathbb{C}$ such that

$$B=\alpha e^{i\theta}A+c=\left\{\alpha e^{i\theta}z+c : z\in A\right\}.$$

The parameters are: α (scale factor), θ (rotation angle), and c (translation vector). We call A the *prototype* and B the *model*.

For geometrically similar sets, the length ratio is $L_r=\alpha$ and the area ratio is $A_r=\alpha^2$. This framework allows us to describe numerical-range distortion in precise geometric terms—when an exact similitude relation actually holds, which, as we shall see, is the exception rather than the rule.

3. Numerical Range Examples

We begin by illustrating the variety of numerical-range shapes through representative examples, following the exposition in [3] [4]. These will serve as test cases for our distortion analysis.

Example 3.1 (Nilpotent matrix, [3] Example 1.3.4). The matrix $T=\begin{pmatrix}0&1\\0&0\end{pmatrix}$ is nilpotent with $T^2=0$. Its numerical range is the closed disk

$$W(T)=\{z\in\mathbb{C}:|z|\le 1/2\}$$

centered at the origin with radius $w(T)=1/2$. More generally, for $T=\begin{pmatrix}0&a\\0&0\end{pmatrix}$

we have $W(T)=\{z:|z|\le|a|/2\}$. This example is fundamental because $W(T)$ is a perfect disk, making distortion effects clearly visible. The set is plotted in Figure 1.

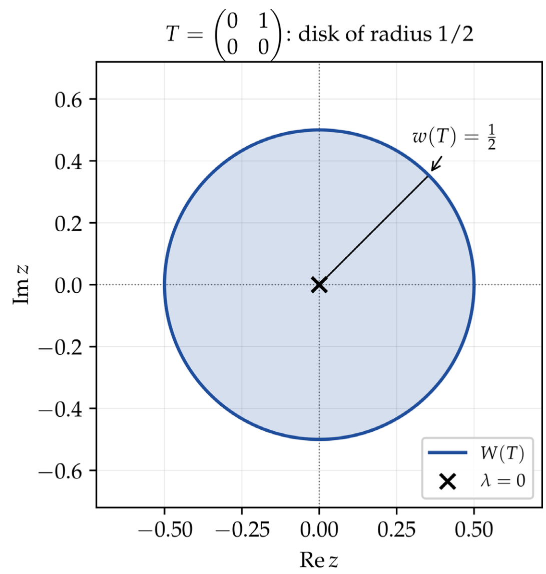

Figure 1. Numerical range of the nilpotent matrix $T=\begin{pmatrix}0&1\\0&0\end{pmatrix}$.

The numerical range is a disk of radius 1/2 centered at the origin. The sole eigenvalue $\lambda=0$ lies at the center.

Example 3.2 (Hermitian matrix, [3] Theorem 1.2.2). For a Hermitian matrix $T=T^*$, all eigenvalues $\lambda_1\le\lambda_2\le\cdots\le\lambda_n$ are real, and

$$W(T)=[\lambda_1,\lambda_n]=[\lambda_{\min}(T),\lambda_{\max}(T)].$$

The numerical range degenerates to a line segment on the real axis, and $w(T)=\max\{|\lambda_1|,|\lambda_n|\}=\|T\|$. Figure 2 illustrates this degenerate case.

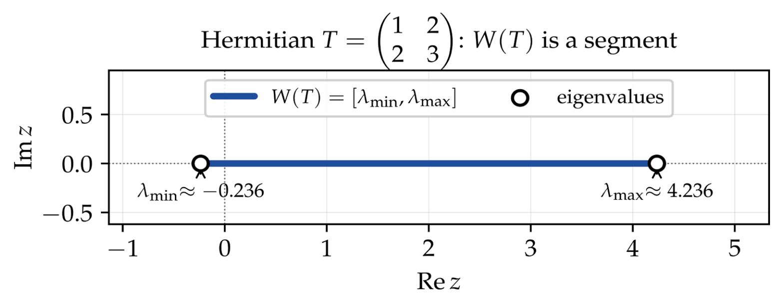

Figure 2. Numerical range of a Hermitian matrix. Since $T=T^*$, all eigenvalues are real and $W(T)$ is the line segment connecting the extreme eigenvalues.

Example 3.3 (Upper triangular matrix, [3] Theorem 1.3.1). For $T=\begin{pmatrix}1&2\\0&3\end{pmatrix}$,

the eigenvalues are $\lambda_1 = 1$ and $\lambda_2 = 3$. By the elliptical range theorem, $W(T)$ is an elliptical disk with foci at 1 and 3. The semi-axes depend on the off-diagonal entry: larger values produce rounder ellipses. See **Figure 3**.

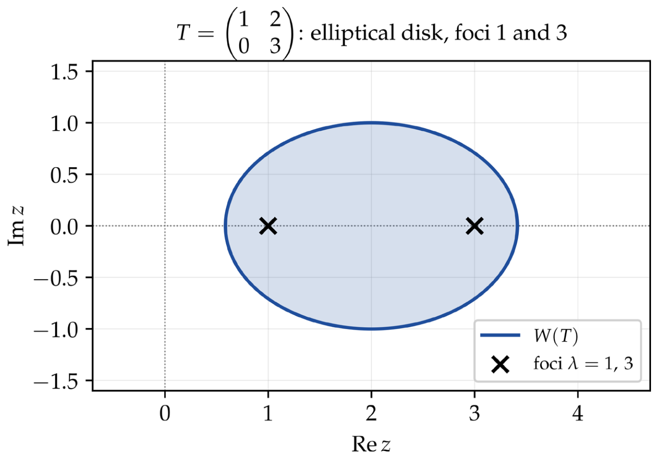

Figure 3. Numerical range of the upper triangular matrix $T = \begin{pmatrix} 1 & 2 \\ 0 & 3 \end{pmatrix}$. The elliptical disk has foci at the eigenvalues $\lambda = 1$ and $\lambda = 3$.

Example 3.4 (3 × 3 matrix). For $n \geq 3$, numerical ranges exhibit richer geometry. The matrix

$$T = \begin{pmatrix} 1 & 1 & 0 \\ 0 & 2 & 1 \\ 0 & 0 & 3 \end{pmatrix}$$

has eigenvalues 1, 2, 3. The numerical range $W(T)$ is a convex set containing these points, with a boundary that may have both flat and curved portions; it is displayed in **Figure 4**.

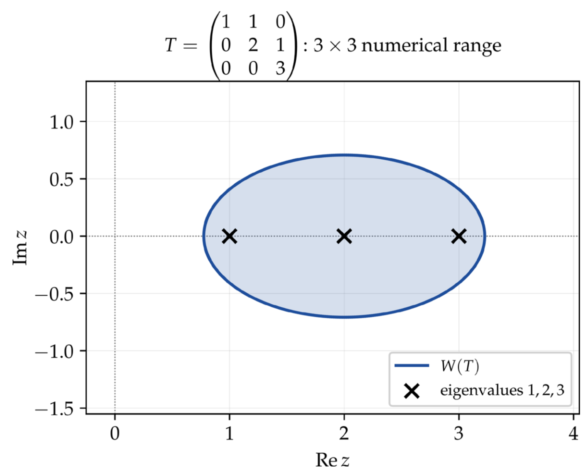

Figure 4. Numerical range of a 3 × 3 upper triangular matrix with eigenvalues at 1, 2, 3. The boundary exhibits curvature characteristic of higher-dimensional numerical ranges.

4. Distortion under Similarity Transformations

We now establish the fundamental results on numerical-range distortion under similarity. Before stating the main theorem, we record two elementary observations and one cautionary example. The example shows that the most naive picture of distortion—a radial dilation of the numerical range by the condition number—is false, and thereby delimits what any correct theorem can assert.

Example 4.1 (No inclusion $W(S) \subseteq \kappa(X) \cdot \mathrm{conv}(W(T))$). Let

$$T = \begin{pmatrix} 1 & 0 \\ 0 & -1 \end{pmatrix}, \quad X = \begin{pmatrix} 1 & 1 \\ 0 & 1 \end{pmatrix}, \quad S = X^{-1}TX = \begin{pmatrix} 1 & 2 \\ 0 & -1 \end{pmatrix}.$$

Here, T is Hermitian, so $W(T) = [-1,1] \subset \mathbb{R}$, and $\kappa(X) \cdot \mathrm{conv}(W(T)) = [-\kappa(X), \kappa(X)]$ is again a subset of the real axis, for any value of $\kappa(X)$. On the other hand, by the elliptical range theorem (Theorem 2.5), $W(S)$ is the ellipse with foci ±1 and minor axis $b = \sqrt{\mathrm{tr}(S^*S) - 2} = \sqrt{6-2} = 2$: a nondegenerate elliptical disk reaching the points $\pm i$ on the imaginary axis. Hence

$$W(S) \not\subseteq \lambda \cdot \mathrm{conv}(W(T)) \text{ for every } \lambda > 0.$$

No scalar multiple of the prototype region can contain the model region: similarity can genuinely change the shape and dimension of the numerical range, not merely its size. Any correct distortion theorem must therefore bound the *size* of $W(S)$—for instance, through the numerical radius—rather than assert a set inclusion into a dilate of $W(T)$.

4.1. The Distortion Bound

The following theorem is our replacement for the set-inclusion statement discussed above. It gives a rigorous, dimension-free bound for the numerical radius of $S = X^{-1}TX$, sharp in the unitary case $\kappa(X) = 1$.

Theorem 4.2 (Numerical radius distortion bound). *Let* $T \in M_n(\mathbb{C})$, *let* $X \in M_n(\mathbb{C})$ *be invertible, and let* $S = X^{-1}TX$. *Then*

$$w(S) \le \left(1 + \kappa(X) - \kappa(X)^{-1}\right) w(T), \tag{2}$$

and consequently

$$W(S) \subseteq \left\{ z \in \mathbb{C} : |z| \le \left(1 + \kappa(X) - \kappa(X)^{-1}\right) w(T) \right\}. \tag{3}$$

Proof. Step 1: *reduction to a positive similarity.* Let $X = UP$ be the polar decomposition, with U unitary and $P = (X^*X)^{1/2}$ positive definite. Then

$$S = X^{-1}TX = P^{-1}(U^*TU)P = P^{-1}T'P, \quad T' = U^*TU,$$

and $w(T') = w(T)$ (unitary invariance), while $\kappa(P) = \kappa(X)$ since P and X have the same singular values. We may therefore assume $X = P$ is positive definite. Moreover, since P and cP induce the same similarity for $c > 0$ and

$\kappa(cP)=\kappa(P)$, we may normalize P so that its spectrum satisfies

$$\sigma(P)\subseteq\left[\kappa^{-1/2},\kappa^{1/2}\right],\quad \kappa:=\kappa(P)=\kappa(X).$$

Step 2: *a constrained bilinear form*. Fix a unit vector y and let $z=\langle Sy,y\rangle\in W(S)$. Since P is self-adjoint,

$$z=\left\langle P^{-1}T'Py,y\right\rangle=\left\langle T'Py,P^{-1}y\right\rangle=\left\langle T'u,v\right\rangle,\quad u:=Py,\quad v:=P^{-1}y.$$

The vectors u,v satisfy the two key constraints

$$\langle u,v\rangle=\left\langle Py,P^{-1}y\right\rangle=\langle y,y\rangle=1,$$

and, by the Kantorovich inequality (Lemma 2.8) applied to $A=P^2$, whose spectrum lies in $\left[\kappa^{-1},\kappa\right]$,

$$\|u\|^2\|v\|^2=\left\langle P^2y,y\right\rangle\left\langle P^{-2}y,y\right\rangle\le\frac{\left(\kappa^{-1}+\kappa\right)^2}{4}.$$

Step 3: *balancing*. For $s>0$, replacing (u,v) by $(u/s,sv)$ changes neither $\langle T'u,v\rangle$ nor $\langle u,v\rangle$. Choosing $s=\sqrt{\|u\|/\|v\|}$ we may assume $\|u\|=\|v\|=\rho$, where

$$1\le\rho^2=\|u\|\|v\|\le\frac{\kappa+\kappa^{-1}}{2},$$

the lower bound following from $1=|\langle u,v\rangle|\le\|u\|\|v\|$ (Cauchy-Schwarz).

Step 4: *orthogonal decomposition*. Write $v=\beta u+w$ with $w\perp u$. Then $\beta=\langle v,u\rangle/\|u\|^2=\overline{\langle u,v\rangle}/\rho^2=\rho^{-2}$, and

$$\|w\|^2=\|v\|^2-|\beta|^2\|u\|^2=\rho^2-\rho^{-2}.$$

Hence

$$z=\langle T'u,v\rangle=\overline{\beta}\langle T'u,u\rangle+\langle T'u,w\rangle=\rho^{-2}\langle T'u,u\rangle+\langle T'u,w\rangle.$$

For the first term, $|\langle T'u,u\rangle|\le w(T')\|u\|^2=w(T)\rho^2$, so

$$\left|\rho^{-2}\langle T'u,u\rangle\right|\le w(T).$$

For the second term, using $\|T'\|=\|U^*TU\|=\|T\|\le 2w(T)$ from (1),

$$|\langle T'u,w\rangle|\le\|T'\|\|u\|\|w\|\le 2w(T)\rho\sqrt{\rho^2-\rho^{-2}}=2w(T)\sqrt{\rho^4-1}.$$

Since $\rho^2\le\left(\kappa+\kappa^{-1}\right)/2$,

$$\rho^4-1\le\frac{\left(\kappa+\kappa^{-1}\right)^2}{4}-1=\frac{\left(\kappa-\kappa^{-1}\right)^2}{4},\ \text{so}\ \sqrt{\rho^4-1}\le\frac{\kappa-\kappa^{-1}}{2}.$$

Combining the two estimates,

$$|z|\le w(T)+2w(T)\cdot\frac{\kappa-\kappa^{-1}}{2}=\left(1+\kappa-\kappa^{-1}\right)w(T).$$

As $z\in W(S)$ was arbitrary, (2) and (3) follow. □

Corollary 4.3 (Two-sided distortion bound). *With* $g(\kappa):=1+\kappa-\kappa^{-1}$ *and the* *hypotheses of Theorem* 4.2,

$$g(\kappa(X))^{-1} w(T) \le w(S) \le g(\kappa(X)) w(T).$$

Proof. The upper bound is Theorem 4.2. For the lower bound, apply Theorem 4.2 to $T = (X^{-1})^{-1} S (X^{-1})$, noting $\kappa(X^{-1}) = \kappa(X)$. □

Remark 4.4. Three comments on the quality of the bound $g(\kappa) = 1 + \kappa - \kappa^{-1}$.

1) At $\kappa = 1$ (*i.e.*, X a scalar multiple of a unitary), $g(1) = 1$ and the theorem recovers the exact unitary invariance $w(S) = w(T)$. The bound is therefore sharp at $\kappa = 1$.

2) The bound always improves the naive estimate obtained from $w(S) \le \|S\| \le \kappa(X)\|T\| \le 2\kappa(X) w(T)$: indeed $g(\kappa) \le 2\kappa - 1 < 2\kappa$ for all $\kappa \ge 1$.

3) The nilpotent example of Section 5 attains the ratio $w(S)/w(T) = \kappa(X)$, so the optimal constant lies between κ and $g(\kappa) = \kappa + (1 - \kappa^{-1})$; the gap is less than 1, uniformly in κ. Extensive numerical experiments (random search over $T, X \in M_n(\mathbb{C})$ for $n \le 5$, and Nelder-Mead optimization of the ratio $w(S)/(\kappa(X) w(T))$ over pairs of complex 2 × 2 matrices, which converges to 1 from below) support the following conjecture.

Conjecture 4.5 (Optimal distortion constant). *For all* $T \in M_n(\mathbb{C})$ *and invertible* $X \in M_n(\mathbb{C})$,

$$w(X^{-1} T X) \le \kappa(X) w(T).$$

By Theorem 5.1 below, the constant $\kappa(X)$ would be optimal.

Remark 4.6. The bound in Corollary 0.16 is a statement about the numerical radius—the size of $W(S)$—and, by (3), about containment of $W(S)$ in a disk. In view of Example 4.1, this is the strongest type of containment statement available at this level of generality: $W(S)$ need not be contained in any dilate of $\operatorname{conv}(W(T))$ itself. The actual scale factor $w(S)/w(T)$ depends on the interplay between the structure of T and the geometry of X; in Section 5, we establish exact formulas for special cases.

4.2. Computational Examples

We illustrate the distortion effect through computed examples.

Example 4.7 (Expansion, $\alpha = 2$). Let $T = \begin{pmatrix} 0 & 1 \\ 0 & 0 \end{pmatrix}$ and $X = \operatorname{diag}(1, 2)$. Then

$$S = X^{-1} T X = \begin{pmatrix} 1 & 0 \\ 0 & 1/2 \end{pmatrix} \begin{pmatrix} 0 & 1 \\ 0 & 0 \end{pmatrix} \begin{pmatrix} 1 & 0 \\ 0 & 2 \end{pmatrix} = \begin{pmatrix} 0 & 2 \\ 0 & 0 \end{pmatrix}.$$

We have $w(T) = 1/2$, $w(S) = 1$, so the scale factor is $w(S)/w(T) = 2 = \|X\|$. The condition number is $\kappa(X) = 2$; the conjectured optimal bound $\kappa(X) w(T)$ is attained exactly, and the proven bound $g(2) w(T) = 2.5 w(T)$ holds with room to spare. Figure 5 compares the two numerical ranges.

Example 4.8 (Contraction, $\alpha = 0.5$). With the same T but $X = \operatorname{diag}(1, 0.5)$, we obtain $S = \begin{pmatrix} 0 & 0.5 \\ 0 & 0 \end{pmatrix}$. Now $w(S) = 0.25$ and $w(S)/w(T) = 0.5$. Note that

$\|X\|=1$ but $\|X^{-1}\|=2$, giving $\kappa(X)=2$. The scale factor $0.5=1/\|X^{-1}\|$ demonstrates that contraction is governed by X^{-1}; see Figure 6.

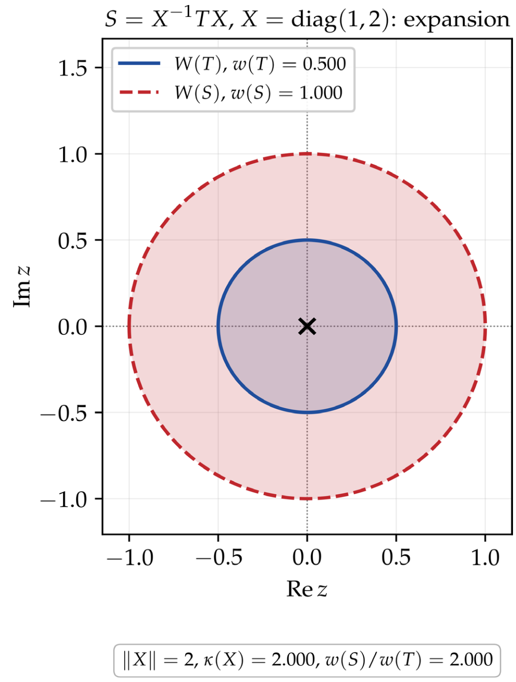

Figure 5. Similarity with $X=\mathrm{diag}(1,2)$: the numerical range expands by factor 2. Blue shows $W(T)$ (prototype), red shows $W(S)$ (model). The scale factor equals $\|X\|=2$.

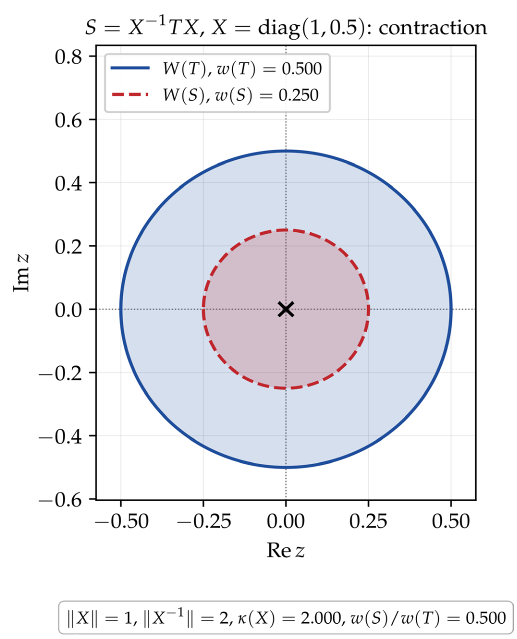

Figure 6. Similarity with $X=\mathrm{diag}(1,0.5)$: the numerical range contracts by a factor of 0.5. The scale factor equals the diagonal parameter α, not $\|X\|=1$.

Example 4.9 (Transpose similarity). For any matrix S, its transpose $T = S^{\mathrm{T}}$ is similar to S; this classical result ([7], Corollary 3.2.4) has implications for numerical ranges. For $S = \begin{pmatrix} 1 & 2 \\ 3 & 4 \end{pmatrix}$, the similarity $T = X^{-1}SX$ with $X = \operatorname{diag}(1, 3/2)$ gives $T = S^{\mathrm{T}}$. Remarkably, $w(S) = w(T) \approx 5.415$, reflecting the fact that $W(S) = W(S^{\mathrm{T}})$ for all matrices, as noted in [6]. This illustrates that the scale factor can be exactly 1 even when $X \neq I$ and $\kappa(X) > 1$; the two coincident numerical ranges are shown in **Figure 7**.

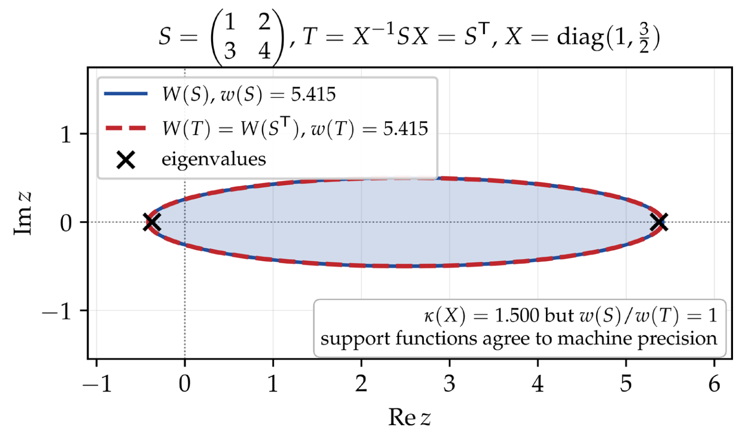

Figure 7. A matrix and its transpose have identical numerical ranges despite being related by a non-trivial similarity. This illustrates that the scale factor can be exactly 1 even when $X \neq I$.

5. Exact Scale Factor for Nilpotent Matrices

Our computational investigations reveal an exact formula for the scale factor in the nilpotent case, demonstrating that the constant $\kappa(X)$ in Conjecture 4.5 is attained.

Theorem 5.1 (Exact scale factor). *Let* $T = \begin{pmatrix} 0 & a \\ 0 & 0 \end{pmatrix}$ *be a* 2×2 *nilpotent matrix with* $a \neq 0$, *and let* $X = \operatorname{diag}(d_1, d_2)$ *with* $d_1, d_2 \neq 0$. *If* $S = X^{-1}TX$, *then*

$$\frac{w(S)}{w(T)} = \left|\frac{d_2}{d_1}\right|.$$

Consequently, $W(S)$ *and* $W(T)$ *are concentric disks with length ratio* $L_r = |d_2/d_1|$ *and area ratio* $A_r = |d_2/d_1|^2$.

Proof. Direct computation yields

$$S = X^{-1}TX = \begin{pmatrix} d_1^{-1} & 0 \\ 0 & d_2^{-1} \end{pmatrix}\begin{pmatrix} 0 & a \\ 0 & 0 \end{pmatrix}\begin{pmatrix} d_1 & 0 \\ 0 & d_2 \end{pmatrix} = \begin{pmatrix} 0 & a\,d_2/d_1 \\ 0 & 0 \end{pmatrix}.$$

By Example 31, the numerical range of $\begin{pmatrix} 0 & b \\ 0 & 0 \end{pmatrix}$ is $\{z : |z| \leq |b|/2\}$ with numerical radius $|b|/2$. Therefore

$$w(T)=\frac{|a|}{2},\quad w(S)=\frac{|a\,d_2/d_1|}{2}=\frac{|a||d_2/d_1|}{2},$$

and the ratio is $w(S)/w(T)=|d_2/d_1|$. □

Corollary 5.2 (Scale-invariant sharpness). *For the nilpotent case with diagonal similarity* $X=\operatorname{diag}(d_1,d_2)$, *we have* $\kappa(X)=\max(|d_1|,|d_2|)/\min(|d_1|,|d_2|)$ *and*

$$\frac{w(S)}{w(T)}=\left|\frac{d_2}{d_1}\right|=\begin{cases}\kappa(X) & \text{if } |d_2|\ge|d_1|,\\ \kappa(X)^{-1} & \text{if } |d_2|\le|d_1|.\end{cases}$$

In particular, the conjectured bound $w(S)\le\kappa(X)w(T)$ *is attained with equality whenever* $|d_2|\ge|d_1|$, *and the lower extreme* $w(S)=\kappa(X)^{-1}w(T)$ *is attained whenever* $|d_2|\le|d_1|$. *Both statements are invariant under rescaling* $X\mapsto cX$ $(c\ne0)$, *as they must be, since* X *and* cX *implement the same similarity. (When* $|d_1|=|d_2|$ *the two cases agree:* $\kappa(X)=1$ *and* $w(S)=w(T)$.)

Proof. Immediately from Theorem 5.1 and

$$\kappa(X)=\frac{\max(|d_1|,|d_2|)}{\min(|d_1|,|d_2|)}:$$

if $|d_2|\ge|d_1|$ then $|d_2/d_1|=\kappa(X)$; if $|d_2|\le|d_1|$ then $|d_2/d_1|=\kappa(X)^{-1}$. □

Remark 5.3. Theorem 5.1 reveals that for nilpotent matrices, the scale factor depends on the ratio of the diagonal entries, not on their individual magnitudes or on the operator norms separately. This geometric insight is obscured by condition-number bounds, which treat expansion and contraction asymmetrically.

Table 1 records the computed scale factors for a range of values of α, and Figure 8 plots them against the prediction of Theorem 5.1.

Table 1. Scale-factor analysis for $T=\begin{pmatrix}0&1\\0&0\end{pmatrix}$ with $X=\operatorname{diag}(1,\alpha)$. The scale factor $w(S)/w(T)=|\alpha|$ exactly, confirming Theorem 5.1. For $\alpha\ge1$ ($|d_2|\ge|d_1|$) the ratio equals $\kappa(X)$; for $\alpha\le1$ it equals $\kappa(X)^{-1}$, in accordance with Corollary 5.2.

α	$\|X\|$	$\|X^{-1}\|$	$\kappa(X)$	$w(S)/w(T)$	$\|\alpha\|$
0.25	1.000	4.000	4.000	0.250	0.25
0.50	1.000	2.000	2.000	0.500	0.50
1.00	1.000	1.000	1.000	1.000	1.00
2.00	2.000	1.000	2.000	2.000	2.00
4.00	4.000	1.000	4.000	4.000	4.00

Limitations of the exact analysis. We emphasize the scope of what has been proved in this section. The exact distortion formula of Theorem 5.1, and the resulting exact similitude between $W(T)$ and $W(S)$, are established only for 2 × 2 nilpotent matrices under diagonal similarity. In this very special situation, both numerical ranges are disks centered at the origin, so size determines shape. For general matrices T and general invertible X, our results (Theorem 4.2, Corollary 4.3) are bounds on the numerical radius, not a geometric classification of $W(S)$: Example 4.1 shows that $W(S)$ may fail to be geometrically similar to $W(T)$ in any sense—indeed, a segment may deform into a genuinely two-dimensional ellipse. Section 9 makes this rigidity phenomenon precise in the 2 × 2 case. A full geometric classification of the possible pairs $\left(W(T), W\left(X^{-1}TX\right)\right)$ for $n \geq 3$ remains open.

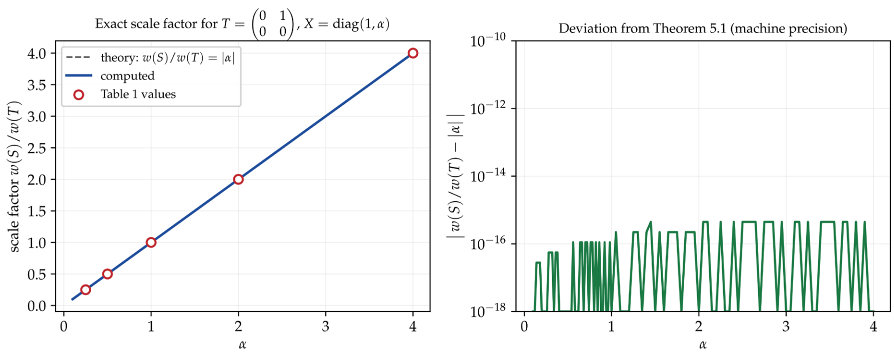

Figure 8. Systematic verification of Theorem 5.1. For each value of α, the computed scale factor $w(S)/w(T)$ equals $|\alpha|$ exactly.

6. Metric Similarity

We now extend our analysis to metric similarity, establishing a fundamental invariance result. Metric similarity, which combines similarity with unitary equivalence, arises naturally in the study of operator algebras and has connections to the polar decomposition [4] [9].

6.1. The Invariance Theorem

Theorem 6.1 (Metric similarity invariance). *Let* $T \in M_n(\mathbb{C})$, *let* X *be positive invertible, and let* U *be unitary. Then*

$$W\left(UX^{-1}TXU^{*}\right) = W\left(X^{-1}TX\right).$$

The unitary component U *has no effect on the numerical range.*

Proof. For any matrix A and unitary U we have $W\left(UAU^{*}\right) = W(A)$: the substitution $y = U^{*}x$ shows that as x ranges over unit vectors so does y, and

$$\left\langle UAU^{*}x, x\right\rangle = \left\langle AU^{*}x, U^{*}x\right\rangle = \left\langle Ay, y\right\rangle.$$

Applying this with $A = X^{-1}TX$ yields the result. □

Corollary 6.2. *For numerical-range analysis, metric similarity and ordinary similarity are equivalent:*

$$S \overset{\text{m.s.}}{\sim} T \;\Rightarrow\; W(S) = W\left(X^{-1}TX\right) \text{ for some positive invertible } X.$$

All results established for similarity in Sections 4-5 apply unchanged to metric similarity.

6.2. Computational Verification

To verify Theorem 6.1 computationally, we tested five different unitary matrices U with the same positive $X = \mathrm{diag}(1,2)$: 1) $U_1 = I$ (identity); 2) $U_2 = \begin{pmatrix} 0 & 1 \\ 1 & 0 \end{pmatrix}$ (permutation); 3) $U_3 = \begin{pmatrix} 1 & 0 \\ 0 & -1 \end{pmatrix}$ (diagonal); 4) $U_4 = \begin{pmatrix} 0 & i \\ i & 0 \end{pmatrix}$ (complex); (v) U_5 a random unitary drawn from Haar measure. In all cases, the computed numerical radius was $w\left(UX^{-1}TXU^{*}\right) = 1.000000$, confirming the theorem. Figure 9 superimposes the numerical ranges obtained under ordinary and metric similarity for $U = U_2$, and Figure 10 reports the outcome for all five unitaries.

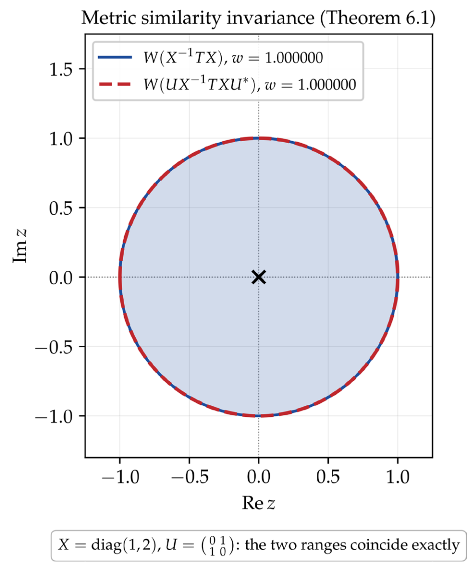

Figure 9. Metric similarity analysis. The numerical ranges $W\left(X^{-1}TX\right)$ (ordinary similarity) and $W\left(UX^{-1}TXU^{*}\right)$ (metric similarity) are identical. The numerical radii satisfy $w\left(X^{-1}TX\right) = w\left(UX^{-1}TXU^{*}\right)$ exactly.

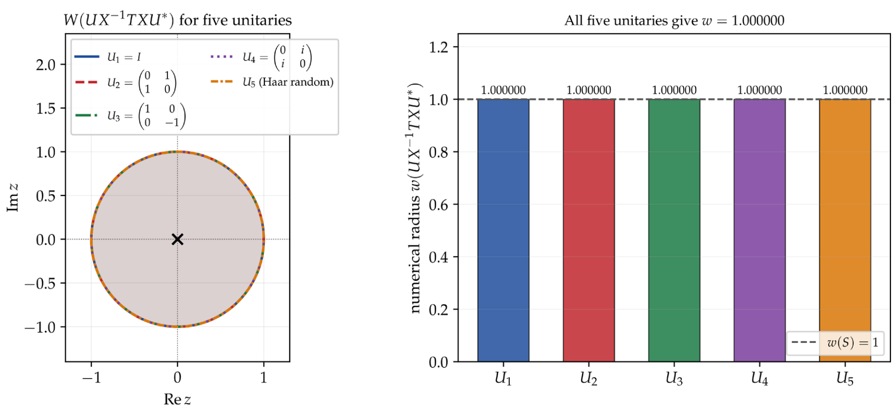

Figure 10. Verification with multiple unitary matrices. All five choices of U produce identical numerical radius $w(S) = 1.0$, confirming that U has no effect on the numerical range.

7. Comparison of Equivalence Relations

We summarize in **Table 2** the effects of the three equivalence relations on key operator-theoretic quantities. This classification extends the systematic study of numerical-range preservers initiated in [6] and connects to the broader theory of operator equivalences in [4].

Table 2. Comparison of equivalence relations and their preservation properties.

Relation	Definition	Spectrum	Num. Range	Num. Radius
Unitary Equivalence	$S = U^* TU$	Preserved	Preserved	Preserved
Metric Similarity	$S = UX^{-1}TXU^*$	Preserved	Distorted	Distorted
Similarity	$S = X^{-1}TX$	Preserved	Distorted	Distorted

The spectrum $\sigma(T)$ is preserved under all three relations because similar matrices have identical characteristic polynomials ([7], Theorem 1.3.20). However, the numerical range, being defined through the inner-product structure, is sensitive to non-unitary transformations [3].

Theorem 7.1 (Distortion hierarchy). *Let* $T \in M_n(\mathbb{C})$ *and let* S *be related to* T *by one of the three equivalence relations. With* $g(\kappa) = 1 + \kappa - \kappa^{-1}$:

(i) *If* $S = U^* TU$ (*unitary equivalence*), *then* $W(S) = W(T)$ *and* $w(S) = w(T)$.

(ii) *If* $S = UX^{-1}TXU^*$ (*metric similarity*), *then* $W(S) = W(X^{-1}TX)$ *and*

$$g(\kappa(X))^{-1} w(T) \le w(S) \le g(\kappa(X)) w(T).$$

(iii) *If* $S = X^{-1}TX$ (*similarity*), *the same bounds hold.*

Proof. (1) is classical; (iii) is Corollary 4.3; (ii) follows from (iii) together with Theorem 6.1. □

The identity $W(UX^{-1}TXU^*) = W(X^{-1}TX)$ shows that metric similarity factors through ordinary similarity for numerical-range purposes. The unitary component affects the eigenvector structure but not the numerical range.

8. The Prototype-Model Framework

Our results admit a natural geometric interpretation through the lens of similitude, connecting to the theory of self-similar sets developed by Hutchinson [10] and the geometric study of convex sets [9].

Definition 8.1. Given $S = X^{-1}TX$, we call $W(T)$ the prototype and $W(S)$ the model. The similarity transformation X induces a quantitative relationship between these sets characterized by:

(i) *Scale factor*: $\alpha = w(S)/w(T)$, which by Corollary 4.3 satisfies

$$g(\kappa(X))^{-1} \le \alpha \le g(\kappa(X)), \quad g(\kappa) = 1 + \kappa - \kappa^{-1}.$$

(ii) *Length ratio*: $L_r = \alpha$ and *area ratio* $A_r = \alpha^2$, whenever $W(S)$ and $W(T)$ are in fact geometrically similar in the sense of Definition 2.9.

For nilpotent matrices with diagonal X, Theorem 5.1 shows that $W(T)$ and $W(S)$ are exact similitudes (concentric disks) with scale factor $|d_2/d_1|$, so the length and area ratios in (ii) are meaningful and computable. In general, however, $W(T)$ and $W(S)$ need not be similar to one another: Example 4.1 exhibits a similarity carrying a line segment to a nondegenerate elliptical disk, and Section 9 shows that for 2×2 matrices with distinct eigenvalues, an exact similitude relation forces $W(S)=W(T)$. Accordingly, in the general case, the prototype-model relationship must be understood through the proven numerical-radius bounds: the model's size is controlled by

$$g(\kappa(X))^{-1}w(T)\le w(S)\le g(\kappa(X))w(T),$$

$$W(S)\subseteq\{z\in\mathbb{C}:|z|\le g(\kappa(X))w(T)\},$$

and not by any radial containment between $W(S)$ and $W(T)$ themselves. In particular, the containments $\kappa(X)^{-1}W(T)\subseteq W(S)\subseteq\kappa(X)W(T)$ asserted in an earlier version of this work are false in general and have been withdrawn; Example 4.1 is a counterexample to both inclusions.

9. The Rotation Question: Partial Results and a Counterexample

For $S=X^{-1}TX$, write

$$\tilde{W}(T)=\frac{W(T)}{w(T)},\quad \tilde{W}(S)=\frac{W(S)}{w(S)}$$

for the numerical ranges normalized to unit numerical radius (assuming $T\ne 0$; note $w(T)=0$ iff $T=0$ iff $S=0$). An earlier version of this work conjectured, on visual evidence, that $\tilde{W}(S)=\mathrm{e}^{i\theta}\tilde{W}(T)$ for some rotation angle θ depending on X. In this section we settle the question completely in the 2×2 case: the conjecture holds—trivially, and with $\theta=0$—for nilpotent T, but fails in general, and we characterize exactly when it holds. The key mechanism is a rigidity phenomenon: because similarity preserves eigenvalues, and eigenvalues are the foci of the elliptical numerical range, an exact similitude relation between $W(S)$ and $W(T)$ is severely constrained.

Proposition 9.1 (Nilpotent case: the conjecture holds with $\theta=0$). *Let $T\in M_2(\mathbb{C})$ be nilpotent, $T\ne 0$, and let X be invertible. Then $S=X^{-1}TX$ is nilpotent, both $W(T)$ and $W(S)$ are closed disks centered at the origin, and*

$$\tilde{W}(S)=\tilde{W}(T)=\overline{\mathbb{D}}.$$

Proof. S is nilpotent since similarity preserves the characteristic polynomial. Every nonzero nilpotent $A\in M_2(\mathbb{C})$ is unitarily equivalent to $\begin{pmatrix}0 & b\\ 0 & 0\end{pmatrix}$ with $b\ne 0$ (Schur triangularization), so by Example 0.10, $W(A)$ is the closed disk of radius $|b|/2$ centered at 0. Normalizing by the numerical radius yields the closed unit disk in both cases. □

Proposition 9.2 (Rigidity for distinct eigenvalues). *Let* $T \in M_2(\mathbb{C})$ *have distinct eigenvalues* $\lambda_1 \neq \lambda_2$, *let* X *be invertible, and let* $S = X^{-1}TX$. *The following are equivalent*:

(a) $W(S) = \alpha e^{i\theta} W(T) + c$ *for some* $\alpha > 0$, $\theta \in [0, 2\pi)$, $c \in \mathbb{C}$ (*i.e.*, $W(S)$ *is a similitude of* $W(T)$);

(b) $W(S) = W(T)$;

(c) $\operatorname{tr}(S^* S) = \operatorname{tr}(T^* T)$.

Proof. (b) $\Rightarrow$ (a) is trivial. For (a) $\Rightarrow$ (b): by Theorem 2.5, $W(T)$ and $W(S)$ are (possibly degenerate) elliptical disks with the same foci $\{\lambda_1, \lambda_2\}$, since $\sigma(S) = \sigma(T)$. A similitude $z \mapsto \alpha e^{i\theta} z + c$ maps an elliptical disk to an elliptical disk and maps foci to foci (also in the degenerate case, where the segment's endpoints are the foci). Hence, the similitude in (a) maps $\{\lambda_1, \lambda_2\}$ onto $\{\lambda_1, \lambda_2\}$. Comparing the distances between the foci gives $\alpha|\lambda_1 - \lambda_2| = |\lambda_1 - \lambda_2|$, so $\alpha = 1$ and the map is an isometry $z \mapsto e^{i\theta} z + c$ fixing $\{\lambda_1, \lambda_2\}$ setwise. If it fixes each focus, then $e^{i\theta}(\lambda_1 - \lambda_2) = \lambda_1 - \lambda_2$ forces $\theta = 0$, $c = 0$, and the map is the identity. If it swaps the foci, then $e^{i\theta}(\lambda_1 - \lambda_2) = \lambda_2 - \lambda_1$ forces $\theta = \pi$ and $c = \lambda_1 + \lambda_2$, *i.e.*, the point reflection through the midpoint $(\lambda_1 + \lambda_2)/2$. An elliptical disk is centrally symmetric about its center, which is the midpoint of its foci; hence, in either case, the image of $W(T)$ is an elliptical disk with foci $\{\lambda_1, \lambda_2\}$ and the same minor axis as $W(T)$. Thus, $W(S)$ and $W(T)$ share foci and minor axis, so $W(S) = W(T)$.

(b) $\Leftrightarrow$ (c): two elliptical disks with the same foci coincide iff their minor axes agree, and by Theorem 2.5, the minor axis of $W(A)$ is $\sqrt{\operatorname{tr}(A^* A) - |\lambda_1|^2 - |\lambda_2|^2}$; since S and T have the same eigenvalues, equality of minor axes is precisely (c). □

Theorem 9.3 (Resolution of the rotation question for $n = 2$). *Let* $T \in M_2(\mathbb{C})$, $T \neq 0$, *let* X *be invertible, and let* $S = X^{-1}TX$. *Then*

$\tilde{W}(S) = e^{i\theta} \tilde{W}(T)$ for some θ $\Leftrightarrow$ T is nilpotent, or $W(S) = W(T)$.

Moreover, whenever the relation holds, it holds with $\theta = 0$: $\tilde{W}(S) = \tilde{W}(T)$.

Proof. ($\Leftarrow$) If T is nilpotent this is Proposition 9.1; if $W(S) = W(T)$ then also $w(S) = w(T)$ and $\tilde{W}(S) = \tilde{W}(T)$.

($\Rightarrow$) Suppose $\tilde{W}(S) = e^{i\theta} \tilde{W}(T)$, *i.e.*,

$$W(S) = \beta e^{i\theta} W(T), \quad \beta := \frac{w(S)}{w(T)} > 0,$$

a similitude with translation $c = 0$, and suppose T is not nilpotent.

Case 1: $\lambda_1 \neq \lambda_2$. Proposition 9.2 applies and gives $W(S) = W(T)$.

Case 2: $\lambda_1 = \lambda_2 = \lambda \neq 0$ (equal eigenvalues; $\lambda \neq 0$ since T is not nilpotent). Write $T = \lambda I + N$ and $S = \lambda I + N'$ with N, N' nilpotent, $N' = X^{-1} N X$. By Proposition 9.1 (or trivially if $N = 0$), $W(T) = \lambda + r_T \overline{\mathbb{D}}$ and $W(S) = \lambda + r_S \overline{\mathbb{D}}$ are disks centered at λ with radii $r_T, r_S \geq 0$. The relation $W(S) = \beta e^{i\theta} W(T)$ forces equality of centers, $\lambda = \beta e^{i\theta} \lambda$, whence $\beta e^{i\theta} = 1$, so $\beta = 1$, $\theta = 0$, and then $r_S = r_T$, *i.e.*, $W(S) = W(T)$.

Finally, in every case where the relation holds we have shown either $\tilde{W}(S)=\tilde{W}(T)=\overline{\mathbb{D}}$ (nilpotent case) or $W(S)=W(T)$; in both, $\theta=0$ works. □

Example 9.4 (Explicit counterexample to the general rotation conjecture). Take $T=\operatorname{diag}(1,-1)$ and $X=\begin{pmatrix}1 & 1\\ 0 & 1\end{pmatrix}$ as in Example 4.1, so $S=\begin{pmatrix}1 & 2\\ 0 & -1\end{pmatrix}$. Then $\tilde{W}(T)=[-1,1]$ is a segment, while $W(S)$ is the elliptical disk with foci ±1 and semi-axes $\sqrt{2}$ (major) and 1 (minor), so $w(S)=\sqrt{2}$ and $\tilde{W}(S)$ is a nondegenerate elliptical disk with semi-axes 1 and $1/\sqrt{2}$. A rotated segment can never equal a two-dimensional ellipse, so $\tilde{W}(S)\neq e^{i\theta}\tilde{W}(T)$ for every θ. (Consistency check: $\kappa(X)=(3+\sqrt{5})/2\approx 2.618$ and $w(S)=\sqrt{2}\leq\kappa(X)w(T)$, in accordance with Conjecture 4.5 and Theorem 4.2.)

Remark 9.5. (Higher dimensions and boundary generating curves). The mechanism behind Proposition 9.2 is that the eigenvalues, which are invariant under similarity, serve as the foci of the boundary of W in the 2 × 2 case. For $n\geq 3$ the natural tool is Kippenhahn's determinantal representation [11]: writing $T=H+iK$ with H,K Hermitian, the numerical range $W(T)$ is the convex hull of the real affine part of the algebraic curve dual to

$$p_T(u,v,w)=\det(uH+vK+wI)=0,$$

and the (real) foci of this boundary generating curve are precisely the eigenvalues of T. Since similarity preserves eigenvalues, any exact similitude between the boundary generating curves of $W(T)$ and $W(S)$ is subject to the same focus-rigidity as in Proposition 9.2. However, for $n\geq 3$ the set $W(S)$ does not determine its generating curve, and a similitude of the convex sets need not extend to a similitude of the curves; a complete classification is therefore open. We record the two questions our analysis leaves open in the form suggested by the $n=2$ resolution.

Open Problem 9.6. Characterize the pairs (T,X), $T\in M_n(\mathbb{C})$, X invertible, for which $W(X^{-1}TX)$ is a similitude of $W(T)$. Theorem 9.3 resolves the case $n=2$: for distinct eigenvalues, this occurs only trivially ($W(S)=W(T)$), while for coincident eigenvalues, it always occurs, with rotation angle 0. We conjecture that also for $n\geq 3$, whenever the similitude relation holds, the rotation angle can be taken to be $\theta=0$ modulo the symmetries of $W(T)$.

10. Conclusions and Future Directions

This paper develops a framework for understanding numerical-range distortion under similarity and metric similarity of matrices, in the tradition of Toeplitz [1], Hausdorff [2], and Goldberg-Straus [8]. Our principal contributions are:

1) Distortion bounds. We proved the two-sided numerical-radius bound $g(\kappa(X))^{-1}w(T)\leq w(X^{-1}TX)\leq g(\kappa(X))w(T)$ with $g(\kappa)=1+\kappa-\kappa^{-1}$ (Theorem 4.2, Corollary 4.3), sharp in the unitary case, and we showed by an explicit example that no set inclusion of the form $W(S)\subseteq\kappa(X)\cdot\operatorname{conv}(W(T))$ can hold in general (Example 4.1). We conjecture that the optimal constant is $\kappa(X)$ (Conjecture 4.5), which is attained on the nilpotent family.

2) Exact formulas. For nilpotent 2 × 2 matrices with diagonal similarity $X = \operatorname{diag}(d_1, d_2)$, we established the exact scale factor formula $w(S)/w(T) = |d_2/d_1|$, with the scale-invariant sharpness dichotomy of Corollary 0.24.

3) Metric similarity invariance. We proved the identity $W\left(UX^{-1}TXU^*\right) = W\left(X^{-1}TX\right)$, showing that the unitary component has no effect on numerical-range distortion; this extends the invariance properties cataloged in [6].

4) Resolution of the rotation question for $n = 2$. We showed that the normalized numerical ranges $\tilde{W}(S)$ and $\tilde{W}(T)$ are related by a rotation precisely when T is nilpotent or $W(S) = W(T)$, and that the rotation angle can then be taken to be zero (Theorem 9.3); the general similitude classification for $n \geq 3$ is posed as Open Problem 9.6, together with the Kippenhahn-curve approach sketched in Remark 9.5.

Limitations. We reiterate the boundaries of the present work. All results are proved for matrices on finite-dimensional spaces; in infinite dimensions, even the spectral inclusion must be modified (Remark 2.4). The exact distortion formula is proved only for 2 × 2 nilpotent matrices under diagonal similarity; for general (T, X) our results are quantitative bounds on the numerical radius rather than a geometric classification of the numerical range, and the optimal distortion constant (conjecturally $\kappa(X)$) remains open. The rotation/similitude question is fully resolved only for $n = 2$.

Beyond Conjecture 4.5 and Open Problem 9.6, natural directions include exact scale factors for larger classes of matrices (e.g., quadratic operators, whose numerical ranges are elliptical), the behavior of the boundary generating curve under similarity for $n = 3$ via Kippenhahn's classification [11], and analogs for the q-numerical range and the numerical ranges of operator polynomials.

Author Contributions

Faith Mwangi was involved in conceptualization, analysis, and writing; Benard Nzimbi and Stephen Luketero were involved in conceptualization and review of the manuscript.

Statement

Computational work was performed using Python with NumPy, SciPy, and Matplotlib.

Conflicts of Interest

The authors declare no conflicts of interest regarding the publication of this paper.

References

[1] Toeplitz, O. (1918) Das algebraische Analogon zu einem Satze von Fejér. *Mathematische*

Zeitschrift, **2**, 187-197. https://doi.org/10.1007/bf01212904

[2] Hausdorff, F. (1919) Der Wertvorrat einer Bilinearform. *Mathematische Zeitschrift*, **3**, 314-316. https://doi.org/10.1007/bf01292610

[3] Gustafson, K.E. and Rao, D.K.M. (1997) Numerical Range: The Field of Values of Linear Operators and Matrices. Springer, 1-26. https://doi.org/10.1007/978-1-4613-8498-4_1

[4] Halmos, P.R. (1982) A Hilbert Space Problem Book. Graduate Texts in Mathematics, 19. 2nd Edition, Springer.

[5] Kittaneh, F. (2005) Numerical Radius Inequalities for Hilbert Space Operators. *Studia Mathematica*, **168**, 73-80. https://doi.org/10.4064/sm168-1-5

[6] Li, C.K. (2001) A Survey on Linear Preservers of Numerical Ranges and Radii. *TJM*, **5**, 477-496. https://doi.org/10.11650/twjm/1500574944

[7] Horn, R.A. and Johnson, C.R. (2012) Matrix Analysis. 2nd Edition, Cambridge University Press.

[8] Goldberg, M. and Straus, E.G. (1977) Elementary Inclusion Relations for Generalized Numerical Ranges. *Linear Algebra and Its Applications*, **18**, 1-24. https://doi.org/10.1016/0024-3795(77)90075-1

[9] Bhatia, R. (1997) Matrix Analysis. Graduate Texts in Mathematics, Vol. 169. Springer.

[10] Hutchinson, J.E. (1981) Fractals and Self-Similarity. *Indiana University Mathematics Journal*, **30**, 713-747. https://doi.org/10.1512/iumj.1981.30.30055

[11] Kippenhahn, R. (1951) Über den Wertevorrat einer Matrix. *Mathematische Nachrichten*, **6**, 193-228. https://doi.org/10.1002/mana.19510060306